



**Manchester
Metropolitan
University**

Gillespie, David and Yap, Moi Hoon and Hewitt, Brett M and Driscoll, Heather and Simanaviciute, Ugne and Hodson-Tole, Emma F and Grant, Robyn A (2019) Description and validation of the LocoWhisk system: Quantifying rodent exploratory, sensory and motor behaviours. *Journal of Neuroscience Methods*, 328. p. 108440. ISSN 0165-0270

Downloaded from: <http://e-space.mmu.ac.uk/624039/>

Version: Accepted Version

Publisher: Elsevier BV

DOI: <https://doi.org/10.1016/j.jneumeth.2019.108440>

Please cite the published version

<https://e-space.mmu.ac.uk>

1 **Description and validation of the LocoWhisk system: Quantifying rodent exploratory,**
2 **sensory and motor behaviours**

3 David Gillespie^a, Moi Hoon Yap^b, Brett M. Hewitt^{b,c,d}, Heather Driscoll^{a,e}, Ugne
4 Simanaviciute^{c,f}, Emma F. Hodson-Tole^g, Robyn A. Grant^{c*}

5

6

7 a School of Engineering, Manchester Metropolitan University, Manchester, UK

8 b School of Computing, Mathematics and Digital Technology, Manchester Metropolitan University,
9 Manchester, UK

10 c School of Science and Environment, Manchester Metropolitan University, Manchester, UK

11 d CSols Ltd, Runcorn, Cheshire, WA7 4QX, UK

12 e Advanced Manufacturing Research Center, University of Sheffield, Sheffield, UK

13 f School of Biological Sciences, University of Manchester, Manchester, UK

14 g Musculoskeletal Science and Sports Medicine Research Centre, Dpt. Lifesciences, Manchester
15 Metropolitan University, Manchester, UK

16

17

18 * Corresponding Author: Robyn.A.Grant: robyn.grant@mmu.ac.uk

19

20

21

22

23

24

25

26

27

28

29

30

31

1 **Abstract**

2 **Background:** Previous studies have demonstrated that analysing whisker movements and
3 locomotion allows us to quantify the behavioural consequences of sensory, motor and cognitive
4 deficits in rodents. Independent whisker and feet trackers exist but there is no fully-automated,
5 open-source software and hardware solution, that measures both whisker movements and gait.
6

7 **New Method:** We present the LocoWhisk arena and new accompanying software (ARTv2) that
8 allows the automatic detection and measurement of both whisker and gait information from high-
9 speed video footage.

10
11 **Results:** We demonstrate the new whisker and foot detector algorithms on high-speed video
12 footage of freely moving small mammals, and show that whisker movement and gait measurements
13 collected in the LocoWhisk arena are similar to previously reported values in the literature.
14

15 **Comparison with existing method(s):** We demonstrate that the whisker and foot detector
16 algorithms, are comparable in accuracy, and in some cases significantly better, than readily available
17 software and manual trackers.
18

19 **Conclusion:** The LocoWhisk system enables the collection of quantitative data from whisker
20 movements and locomotion in freely behaving rodents. The software automatically records both
21 whisker and gait information and provides added statistical tools to analyse the data. We hope the
22 LocoWhisk system and software will serve as a solid foundation from which to support future
23 research in whisker and gait analysis.

24

25

26

27

28

29

30

31

32

33

34

35 **Keywords:** locomotion, whisking, automated tracking, software development, image processing

36

1 Introduction

2 Many small laboratory mammals (rats, mice, guinea pigs, shrews, opossums) rely on their whiskers
3 as their primary sense to guide locomotion and environmental exploration (Arkley et al., 2014;
4 Mitchinson et al., 2011; Grant et al., 2009; Grant et al., 2018a). While the whisker system is an
5 established model for cortical sensory pattern formation and information processing, recent
6 advances in measuring whisker behaviours have enabled it to be suggested as a candidate for also
7 measuring motor control (Grant et al., 2014; Garland et al., 2018). Aspects of whisker movements
8 can also be reliably affected during a variety of sensory, motor and cognitive disorders
9 (Simanaviciute et al., in this issue), including rodent models of Amyotrophic Lateral Sclerosis
10 (Grant et al., 2014), anxiety (Grant et al., 2016), Huntington's disease (Garland et al., 2018) and
11 Alzheimer's disease (Grant et al., 2018b). In the case of Huntington's disease and Alzheimer's
12 disease, mice revealed whisker movement deficits earlier than any other motor behaviour test,
13 including gait assessments (Garland et al., 2018). This demonstrates the utility of measuring whisker
14 movements to quantify motor and cognitive declines.

15 Freely available computer vision libraries (such as OpenCV (Bradski and Kaehler, 2008)) have allowed
16 for the development of several automated rodent whisker trackers, which measure whisker
17 movements from high-speed video. These include: i) WhiskerTracker, which requires infrared-
18 lighting to identify eye positions (Knutsen et al., 2005); ii) an unsupervised tracker (Voigts et al.,
19 2008), which can track a single row of whiskers when all the other whiskers have been trimmed; iii)
20 Whisk, which has been designed for a head-fixed set-up (O'Connor et al., 2010; Clack et al., 2012); iv)
21 Whiskerman (Bale et al., 2015) which tracks and extracts parameters from a single whisker
22 automatically where other whiskers are present and not trimmed; and v) the BIOTACT Whisker
23 Tracking Tool (BWTT) (Perkon et al., 2011), which is only semi-automated, and settings cannot be
24 readjusted through the video to account for areas of high or low brightness and contrast. These
25 whisker trackers have been created by researchers and made freely available (Clack et al., 2012;
26 Knutsen et al., 2005; Perkon et al., 2011); however, there does not yet exist a robust, fully-
27 automated whisker tracker, that can detect whiskers within an intact whisker field in freely moving
28 animals.

29 Foot tracking software exists that tracks and records gait information for rodents, including the
30 Catwalk XT (Noldus Information Technology BV, Wageningen, The Netherlands), MouseWalker
31 (Mendes et al., 2015) and AGATHA (Kloefkorn et al., 2017). However, these systems often require
32 two views (below and side-on), very specific and expensive experimental set-ups (such as the
33 Catwalk XT) and the feet to be clearly imaged, preferably in colour. These software packages rarely
34 work with videos that have been imaged to be used for whisker tracking (i.e. low contrast,
35 monochrome videos). Therefore, it is not possible to conduct whisker and foot tracking together.
36 Used in tandem with locomotion (an established behavioural measure), whisker movements could
37 give an added dimension to quantifying motor control, since these are closely coupled during
38 development (Grant et al., 2012). In addition, it has also been demonstrated that whisker
39 movements can be linked to an animal's locomotion speed, and adjusted according to their
40 environmental experience and attention (Arkley et al., 2014). Therefore, locomotion and whisker
41 movements are closely linked and should be studied in tandem.

42 This has prompted the development of the LocoWhisk system, that can simultaneously measure and
43 quantify rodent whisker and locomotion movements. The primary ambition of the LocoWhisk
44 system is to provide a new, non-invasive assessment of animal health and welfare, through the
45 provision of open-source software and hardware to quantify rodent whisker and locomotion

1 movements. In this article, we introduce new methods for automatically detecting whiskers and feet
2 in small mammals for use with the LocoWhisk arena, and also validate these detection algorithms.
3 For the whisker detector we evaluate its performance against state-of-the-art software, and for the
4 foot detection algorithm it is validated against the ground truth that we produced from manual
5 annotations.

6 **Methods**

7 *LocoWhisk Arena*

8 The LocoWhisk arena is a bespoke, low cost hardware system that enables monochrome high-speed
9 video footage to capture the whiskers and feet simultaneously. The LocoWhisk arena consisted
10 of an aluminium support frame, made of Bosch Rexroth compatible profiles (Figure 1a). These
11 profiles enclosed a glass plate floor, and supported a Perspex arena. The glass plate (6 mm thick) was
12 edged with a strip of 12 V red LEDs (60-100 lumen per metre at 625 nm) around its perimeter,
13 creating a pedobarograph. Clear float glass was selected for the pedobarograph for its high
14 transmission index (Corr et al., 1998). Red LEDs were used as rodents are less sensitive to red light
15 (Dauchy et al., 2015; Peirson et al., 2018). The glass pedobarograph floor was enclosed by sections
16 of Bosch Rexroth compatible profiles, connected to the support frame with a hinge. The floor could
17 be inclined up to 30 degrees (Figure 1a), although all recordings were made on a flat floor in this
18 study (at zero degrees).

19 Animals were placed into a Perspex arena (300x500x150 mm for rats, and 300x200x120 mm for the
20 mice and other species). The arena had a hinged lid, and open bottom, so animals directly contacted
21 the pedobarograph floor with their feet. Contact between the animals' feet and the glass plate
22 disrupted the total internal reflection of the red light. When a foot contact was made with the
23 pedobarograph, the contacting area lit up and could be viewed beneath the feet when filmed from
24 below. The intensity of the light is proportional to the pressure applied. When no foot contact was
25 made with the surface of the pedobarograph, the red lights internally reflected through the glass,
26 and as such could not be seen when viewed from below. Pedobarographs often require a layer of
27 textured paper for surface contact to cause a change in the refractive index of the glass; this was not
28 required for the animals as the surface profile of their feet was sufficient to give rise to the
29 pedobarograph effect. This was of benefit for the LocoWhisk arena as it enabled the whiskers to still
30 be visible while simultaneously imaging the feet.

31 To image the whiskers, a high-speed, high-resolution video camera (Phantom Miro ex2) was
32 positioned below the floor, filming at 500 fps at 640x480 pixels. An infrared light slate (PHLOX SLLUB
33 Backlight 850 nm) was placed on top of the arena to illuminate the whiskers. Multiple video clips
34 were collected opportunistically (by manual trigger) when each animal passed in to the view of the
35 camera, and ranged from 0.6 to 1.6 s in length. Recording stopped when the camera memory was
36 full or the animal stopped exploring. All videos were saved in Audio Video Interleave (avi) format and
37 uploaded to the LocoWhisk ARTv2 software, which automatically selected trackable videos and
38 frames. Trackable videos and frames were identified as when the mouse's head, was clearly shown
39 in the image, and when the mouse was not rearing, which obscured the nose tip (as per Hewitt et
40 al., 2016; Grant et al. 2014).

41 To validate and measure the accuracy of the whisker detector algorithm, video footage was used
42 that had been previously recorded in Grant et al. (2013) and Grant et al. (2018a). Video clips were
43 randomly selected for tracking and included 9 clips of brown rats (*Rattus norvegicus*), 36 clips of
44 house mice (*Mus musculus*), 1 clip of harvest mouse (*Micromys minutus*), and 4 clips of a gray short

1 tailed opossum (*Monodelphis domestica*). The opossum was kept and filmed at the university of
2 Trieste, Italy, and all other species were filmed at the Wildwood Trust in Kent, UK. All animals were
3 adult, and a mixture of males and females were used, animals were assumed to be sexually
4 monomorphic.

5 To trial the arena, whisker outputs and foot detector algorithm, 4 adult brown rats (*Rattus*
6 *norvegicus*) and 2 adult wood mice (*Apodemus sylvaticus*) were tested at the Wildwood Trust, Kent.
7 4 video clips were analysed from rat and 3 from mice for the validation of the foot detector and
8 software outputs. All procedures were approved by the local ethics committees at the Wildwood
9 Trust, University of Sheffield, University of Trieste and Manchester Metropolitan University, in
10 accordance with regulations issued by the UK Home Office.

11 *Software*

12 The software associated with the LocoWhisk arena, has been added to the existing ART software
13 (Hewitt et al., 2018) and will be referred to in this article as ARTv2. ART is an Automated Rodent
14 Tracker capable of generating qualitative and quantitative data of rodent movement and
15 exploration, as well as tracking the distance and speed of the rodent movements (Hewitt et al.
16 2018). ARTv2 is an expansion of this software, building upon the qualitative and quantitative
17 information generated in ART to incorporate whisker movements and gait measurement, as the
18 animal moves within the LocoWhisk arena. It follows the same ethos as ART, being open-source and
19 able to provide similar or better accuracy for whisker tracking than commercial software with
20 minimal user interactions. It is also possible to use previous videos processed by ART to attempt to
21 detect whiskers and foot information within the clip.

22 *Whisker Detection Algorithm*

23 The whisker detection algorithm incorporated into ARTv2, combined several image-processing
24 techniques to enhance the whiskers and separate them from background noise. As whiskers can be
25 difficult to detect against the background of the LocoWhisk arena, a region of interest (ROI) was
26 extracted from the image with a minimal amount of other objects or artefacts in the scene. The ROI
27 was defined as the region between 5% to 20% of the resolution outwards of the animal contour
28 (Figure 2a). This was to avoid noise generated from the immediate surroundings around the animal,
29 and to cover a significant amount of whiskers. A circular segment was added to exclude the nosetip
30 from the binary mask. This mask was then used to extract the ROI from the original image as shown
31 in Figure 2b.

32 With all the background objects removed from the scene, the ROI was then inverted, and pre-
33 processed by linear normalisation (Rosenfeld, 1976) as in Equation 1, where ROI is denoted as I ,
34 $newMin$ is the minimum pixel value and $newMax$ is the maximum of the pixel value detected within
35 the image I . Pixel value is the greyscale pixel intensity value, and Min and Max are defined as the
36 minimum and maximum pixel value of an image, which are 0 and 255 respectively for 8-bit images.
37 I_N was then calculated using Equation 2.

$$I: \{X \subseteq R^n\} \rightarrow \{Min \dots Max\} \quad (1)$$

$$I_N = (I - Min) \frac{newMax - newMin}{Max - Min} + newMin \quad (2)$$

38

1 The equalisation was kept linear as any other form of equalisation introduced too much noise into
 2 the image and created additional line-like segments (Figure 2c). A threshold value was calculated as
 3 the mean pixel intensity of the image, and every pixel from the source image (defined as *src* in
 4 Equation 3) below this value was thresholded to zero (Gonzalez and Woods, 2002) (Equation 3). This
 5 process was repeated with an increasing threshold value, until the mean intensity of the masked
 6 image fell below 10% of the bit depth (25 intensity, for 8-bit images) (Figure 2d). This handles images
 7 of varying brightness, and ensures noisy parts of the image are not picked up as potential whisker
 8 locations.

$$9 \quad dst(x, y) = \begin{cases} src(x, y), & \text{if } src(x, y) > threshold \\ 0, & \text{otherwise} \end{cases} \quad (3)$$

10 After the image was thresholded with equation 3, the whiskers were enhanced, but also shown as
 11 several pixels wide (Figure 2d), with some noise still present. In order to highlight the whiskers
 12 further, probable whisker locations were located. This was done by repeating the process as above,
 13 but instead of using a mask constructed of an inner and outer extension, a mask of only 1 pixel in
 14 width was constructed for all values between the inner and outer extension distances. For each
 15 mask, a Gaussian filter was applied to remove noise and to create a “smoother” gradient profile of
 16 the pixels. Non-maxima suppression (Devernay, 1995) was then applied to the entire kernel, rather
 17 than in a specified direction, to leave only the largest intensity pixel. The size of the kernel was a
 18 trade-off between sensitivity and specificity. Kernel size was determined as 2% of the resolution. The
 19 resulting pixels can be considered a probable location for a whisker position. The process was
 20 repeated several times with the contour being extended by a further pixel each time, leaving an area
 21 several pixels wide with probable whisker locations shown in Figure 3a. A median subset of the
 22 extension distances was chosen to look for the final whisker locations.

23 Each pixel from the non-maxima suppressed image was chosen, and a line mask was created for
 24 every angle (0 - 180°), the length of which was kept short so curved whiskers could still be
 25 approximated by a straight line. This mask was then applied to an image consisting of the potential
 26 whisker locations (Figure 3a) and added to the original extracted image (Figure 3b). The probable
 27 whisker locations increase the intensity considerably, thus giving a much larger mean value when
 28 one of the orientations falls in the correct position. If the mean intensity increased above a certain
 29 pixel value threshold of grayscale intensity (112 pixel value), then the orientation with the largest
 30 response was saved for that pixel. The previous step will have generated several potential whisker
 31 locations (Figure 3c), some of which will be for the same whisker, it was therefore necessary to
 32 reduce these potential locations to just one for each whisker (Figure 3d). The median extension
 33 distance from the subset (15 in this case) was then chosen as the point to determine if the current
 34 pixel was actually a whisker and if the orientation was correct. All potential whisker lines within a 7 ×
 35 7 area were selected. If the point was a whisker, it can be expected that several lines will have been
 36 found in the surrounding area, all with a similar angle. If the number of lines fell below a certain
 37 threshold (50% of the extended ranges, 4 in this case), then it was instantly discarded. If there were
 38 4 or more lines, they were ordered by their angle. The first and last 25% were removed to remove
 39 any large outliers, then the line with the largest mean intensity value was chosen to represent the
 40 whisker, while all other lines were suppressed (Figure 3d). This approach works well in practice, but
 41 a limitation may be that whiskers that are extremely close together will only be identified as one
 42 whisker. While the detection process achieved a very high true positive rate, it also generated a
 43 significant amount of false positives. In order to reduce the false positives, rule-based logic was
 44 applied to each detected whisker, such that if the whisker was found to be parallel to the orientation
 45 of the rodent's face, it was removed. This approach consistently left true positive whiskers.

1 As the whisker detection algorithm is a part of ARTv2, it is possible to export various statistics and
2 measurements about the animal in the clip. The outputs are documented in Table 1, and include
3 whisking frequency, whisker angle, protraction and retraction speed, spread and amplitude of the
4 whiskers. The mean whisker angular position is one of the most important metrics calculated in
5 ARTv2 that the other outputs rely on. It is defined in this paper as the angle between the centre line
6 of the rodents head and the tangent to a given point on a whisker shaft, as shown in Figure 4 and is
7 used in multiple studies (Perkon et al., 2011; Clack et al., 2012; Pammer et al., 2013; Ahissar and
8 Knutsen, 2008; Sofroniew et al., 2014).

9 *Foot detection algorithm*

10 The foot detection algorithm combined several image-processing techniques to detect rodent feet,
11 label the front and hind feet on either side of the body, and also persistently track each identified
12 foot through a video. This was accomplished in two phases, one to detect the feet, while the second
13 phase automatically labelled and tracked the correct foot.

14 Due to rodents being very small and light, and priority given to imaging the whiskers, it can be
15 difficult to detect foot placements from the LocoWhisk arena pedobarograph. In order to clearly
16 highlight the feet of the rodent, the input image was converted to log colour space, as can be seen in
17 Figure 5. This image, in combination with the animals body contour (which is processed as part of
18 ARTv2 and detailed in Hewitt et al. (2018), was used to create a mask which was eroded using
19 OpenCV's erode function (Bradski and Kaehler, 2008). This erosion function removes visual artefacts
20 so that only the feet can be seen, as displayed (Figure 5b.). Any foot that lies outside the body
21 contour is not recorded. The resolution of the mask was then reduced to remove visual artefacts and
22 allow for foot contours to be more easily detected. The mask was processed by the OpenCV
23 findContour (Bradski and Kaehler, 2008) function, to provide a bounding box and a centre point for
24 each foot (Figure 5d).

25 To identify which foot is which, two points were created to split the animal into a left and right side.
26 This is accomplished by using the central point of the body contour and an angle to create the head
27 point and a point between the tail and centroid point (Figure 5, e.). The angle is taken from the angle
28 between the centre point position and the nose tip recorded with ARTv2 (Hewitt et al., 2018) using
29 the inverse arctangent formula. If no nose tip points are available, the angle is calculated by taking
30 the angle between the centroid point in the current frame and a centroid point captured in a
31 subsequent frame using the inverse arctangent formula.

32 With the created points, it was then possible to calculate the perpendicular distance from the cross
33 product between the head point to the centroid position and the foot point to the centroid position.
34 The parallel distance was also calculated from the dot product between these points. If the
35 perpendicular distance was positive, the foot lies on the right side, otherwise it lies on the left side. If
36 the parallel distance was greater than one fifth of the distance to the head point, it is labelled as a
37 front foot, otherwise it is labelled as a hind foot.

38 To persistently track each foot, every frame of the video is inspected for contours; if there are any
39 they are assigned to either an existing or a new identifier. The identifier contains a unique ID with
40 bounding box and centre position. If there no identifiers are stored within the software, the
41 bounding box is registered and the correct foot identifier is calculated. However, if there are
42 registered identifiers, instead of assigning a new ID, we determine if we can associate the foot
43 contour with one of the existing identifiers. This is accomplished by computing the Euclidean
44 distance between the centre points of the new contours, and existing identifiers centre points. We

1 associate new contours that have the minimum distance to the existing identifier, and update its
 2 values for that frame. However, if there is a contour, that is not close to any of the existing points, it
 3 is registered as new foot identifier. To handle identifiers that are no longer discoverable after a
 4 certain number of frames, such as when the animal lifts its foot, the identifier is deregistered after a
 5 certain amount of frames. This is set as 2 frames in the software (i.e. 4 ms at 500 fps) but can be
 6 manually adjusted by the user.

7 After all of the frames have been processed to detect feet, each individual foot is post processed to
 8 remove erroneous data (such as feet recorded to be placed for less than 15 frames). ARTv2, is then
 9 able to export the stride length, swing time and stance time for each individual foot as can be seen
 10 in table 1. It is also possible with other recorded measurements results to be able to calculate other
 11 statistics, such as swing and stance speed, stride distance or pressure placed upon the
 12 pedobarograph (Mendes et al., 2015).

13 *LocoWhisk System outputs*

14 Once the whiskers and feet have been identified with visual indicators to allow users to inspect the
 15 detected whiskers, feet and body contour, it is possible to export various outputs from the software.
 16 The ARTv2 software currently exports 4 output files in comma separated values (.CSV) format, 2 are
 17 general statistics and 2 are mean data for whisker and feet detection, respectively. Table 1 contains
 18 the outputs and the definitions of how each variable is calculated.

19 **Table 1:** The outputs that are calculated by ARTv2 for each clip and on a frame-by-frame basis.

Variable Name	Description
Measures per Clip: Each variable is the mean for each clip and calculated for both left and right side.	
Whisker movement measures:	
Mean Angle (Deg)	The average whisker angular positions from all tracked whiskers.
Frequency (Hz)	An auto-correlogram of the left and right angular positions.
Retraction Speed (Deg/s)	Average retraction velocity (backward moving whiskers) from the angular positions.
Protraction Speed (Deg/s)	Averaged protraction velocity (forward moving whiskers) from the angular positions.
Spread (Deg)	The Standard Deviation of all tracked whiskers.
Amplitude	The Standard Deviation of the angular positions, multiplied by $2 \times \sqrt{2}$ as suggested in (Grant et al., 2014)
Asymmetry	Left minus right mean whisker angles.
Gait measures:	
Stride Distance(mm)	The mean Euclidean distance between individuals foot placements.
Stance Time (ms)	The amount of time that the foot is placed on the floor.
Swing Time (ms)	The amount of time that the foot is lifted in the air.

Variable Name	Description
Measures per frame:	Variables that are provided on a frame-by-frame basis for each clip, for the left and right side.
Whisker and head measures:	
Nose point coordinates	The X,Y coordinates of the nose point.
Mid Head point coordinates	The X,Y coordinates of the midpoint of the head.
Mean whisker Angle	The mean angular position from all tracked whiskers.
Whisker points arrays	An array of the whisker points that were detected in ARTv2.
Gait measures:	
Centroid point of the foot	The centre point of the bounding box for each foot.
Foot Dimensions	The width and height of each foot.
Bounding box of the foot	The coordinates of the bounding box, for each foot is stored for each frame.

1

2 *Validation of whisker detection*

3 To evaluate the performance of ARTv2's whisker detection algorithm, one image was extracted from
4 the video data (50 in total) of many small mammal species performing locomotion and exploration
5 of static objects placed within the set up. The ability of ARTv2 to detect whiskers was measured by
6 counting how many whiskers were correctly detected (True Positive (*TP*)) in 50 selected frames
7 (images) from the collected videos. To compare ARTv2 to existing trackers, Whisk and BWTT were
8 also run on the same 50 images. The number of whiskers detected by Whisk and BWTT were
9 identified, again, by counting the number of true whiskers detected for each tracker. Manual
10 inspection was used to ensure that the detected whiskers were *TP* detections, and only *TP*
11 detections were reported for each tracker. True negative values were unable to be obtained due to
12 the nature of the images, as this would cover almost the entire ROI and would skew the accuracy
13 results.

14 Manual annotations (i.e. MWA, Hewitt et al. 2016) and trackers (ARTv2, Whisk, BWTT) all have
15 different standards of whisker identification. They use different methods of identification; this
16 means that they identify different whiskers as well as different lengths and shapes (curves) of each
17 whisker. Therefore, it was not possible to fairly compare the pixel tracking values between the
18 software (i.e. by using an Intersection over the Union (*IoU*) score). Therefore, only the number of
19 accurately *TP* detected whiskers was recorded for this study.

20

21 *Validation of foot detection*

22 To validate the foot detector in ARTv2, an Intersection over the Union (*IoU*) score was calculated
23 measuring the overlap between predicted foot and ground truth foot annotations. *IoU* is a
24 commonly used metric for object detection (He et al., 2017; Redmon et al., 2016; Lin et al., 2017).
25 Any algorithm that provides predicted coordinates can be evaluated using *IoU*. *IoU* is calculated

1 using equation 4, which measures the area of overlap between the predicted and ground truth
2 coordinates and dividing by the area encompassed by both a ground truth (manual annotation, or a
3 validated ground truth dataset) and predicted outputs (Real and Vargas, 1996).

$$4 \quad J(A,B)= (|A \cap B|)/(|A \cup B|)= (|A \cap B|)/(|A|+|B|-|A \cup B|) \quad (4)$$

5 For foot detection validation, 20 images were selected from our existing database of whisker videos
6 from Brown Rats (*Rattus norvegicus*) (n= 10 images), and wood mice (*Apodemus sylvaticus*) (n=10
7 images), as these are representative of common laboratory animal feet. Specifically, to evaluate the
8 performance of the foot detector, an *IoU* score was computed using the predicted bounding boxes
9 from the foot detector versus ground truth bounding boxes. The selected images were converted to
10 the Log colour space, and then annotated using the Supervisely tool (Supervise.ly, 2019) to create
11 ground truth bounding boxes for each foot. The bounding boxes, were predicted in the software,
12 using different settings for the mice and rats. The settings used to capture the rat feet predictions
13 included: down sampling the created mask twice, eroding the mask fourteen times with a 3x3
14 kernel, and excluding any bounding box, with an area less than 60 pixels. As mice feet are a lot
15 smaller and the mice were a lot lighter, the settings were different. The mask was down sampled
16 once, eroded three times with a kernel size of 3x3 to remove visual errors and bounding boxes were
17 excluded with an area less than 10 pixels. Due to the varying nature of the parameters used within
18 the foot-tracking algorithm (image pyramid, erosion, joining contours together, excluding any area
19 outside the animals contour), a complete match to the ground truth boxes is highly unlikely. *IoU*
20 was chosen to evaluate the foot tracking algorithm as it rewards predicted bounding boxes that
21 overlap with ground truth annotations (He et al., 2017). An *IoU* score greater than 0.5 is normally
22 considered a good prediction (He et al., 2017).

23 **Results**

24 *Whisker detection results*

25 The mean number of whiskers (*TP*) detected for ARTv2 in 50 images was 15.84 ± 5.9 (n=50) (Table
26 2). The mean number of whiskers (*TP*) detected per image for Whisk was 6.8 ± 6.97 (n=50). ARTv2
27 found significantly more whiskers than Whisk (Wilcoxon Signed Rank: $Z=-6.0927$, $p<0.01$) across the
28 same dataset. The mean number of whiskers detected for BWTT was 14.76 ± 4.7 (n=50). Although
29 the *TP* detection rate for ARTv2 was slightly higher, there was no significant difference between the
30 trackers (Wilcoxon Signed Rank: $Z=-1.0554$, $p=0.2891$).

31 Although ARTv2 did not significantly improve upon BWTT over the full dataset, its success was
32 largely dependent on the resolution of the whiskers or “zoom level”. Some videos showed a larger
33 animal, or an animal that was much closer to the camera, and therefore showed the whiskers with a
34 higher spatial resolution (Z1), whereas others recorded a smaller animal, or an animal that was
35 further away (Z2). ARTv2 performed consistently against all zoom levels, although it performed
36 significantly better on videos with high spatial resolution of the whiskers, than BWTT on the Z1
37 dataset (Wilcoxon Signed Rank: $Z=-2.6672$, $p<0.001$, n=13), whereas there was no significant
38 difference on videos with lower spatial resolution on the Z2 dataset. as shown in Table 2, Figure 6.
39
40

41

42

1 **Table 2.** Results table showing the score (compared to manual tracking), mean number of correct
 2 detections, degree of automation, and the number of settings required for each method.

Method	Mean No. of whiskers detected			Automation	Dynamic Settings
	All (n=50)	Z1 (n=13)	Z2 (n=37)		
ARTv2	15.84	22.62	13.5	Fully automated	Calculated per frame
Whisk	6.8	16.69	3.32	Fully automated	Calculated per frame
BWTT	14.76	17.23	13.89	Manual settings at start-up	Calculated on one frame and propagated through clip

3

4 *Foot detection results*

5 The mean *IoU* score for the foot tracking algorithm over the 20 images was 0.502 ± 0.24 std (n=20).
 6 The foot detector itself had a mean *IoU* score of $0.59 (\pm 0.177)$ std, n=10) for rats and $0.37 (\pm 0.261)$
 7 std, n=10) for mice.

8

9 *Locowhisk System Outputs*

10 Table 3 contains a summary of the statistics recorded by ARTv2 for the rats and mice for the same
 11 clips used during the foot tracking validation (above). Mice moved their whiskers with higher
 12 frequency, lower amplitude, and their whiskers were more spread out than rat whiskers (Table 3). As
 13 mice tend to be much faster and are smaller than rats, all locomotion measures for mice were lower
 14 than those of the rat (Table 3).

15 **Table 3:** Mean whisker and gait statistics recorded using ARTv2.

Measures per clip	Rats (n=4) (\pm std)	Mice (n=3) (\pm std)
Whisker movement measures:		
Frequency (Hz)	11.04 ± 5.08	19.49 ± 8.02
Mean Angle (Deg)	84.99 ± 13.36	83.74 ± 10.73
Retraction Speed (Deg/ms)	1.274 ± 0.51	1.535 ± 0.79
Protraction Speed (Deg/ms)	1.434 ± 0.68	0.963 ± 0.41
Spread (Deg)	16.21 ± 2.40	20.95 ± 1.01
Amplitude	24.2 ± 9.30	17.36 ± 4.47
Gait measures:		
Fore Feet Stride Distance (mm)	101.5 ± 42.0	56.95 ± 10.3
Hind Feet Stride Distance (mm)	48.52 ± 0.0	51.42 ± 13.93
Fore Feet Stance Time (ms)	302.0 ± 89.75	131.7 ± 34.38
Hind Feet Stance Time(ms)	365.4 ± 248.7	171.3 ± 72.28
Fore Feet Swing Time (ms)	385.2 ± 130.8	498.3 ± 374.0
Hind Feet Swing Time (ms)	476.0 ± 260.3	216.3 ± 40.42

16

1 Discussion

2 This paper presents the LocoWhisk system that enables the non-invasive assessment of rodent
3 exploratory behaviour by measuring rodent whisker and locomotion movements. It provides the
4 methods and validation of the software (ARTv2), and demonstrates that these are robust and
5 accurate when compared to other trackers or manual alternatives.

6 *Whisker detection*

7 The whisker detector algorithm incorporated into ARTv2, performed similarly to BWTT and better
8 than Whisk. Indeed, Artv2 outperformed Whisk on the detection rate for all whiskers, the *TP* rate
9 was significantly higher for the Z2 dataset when compared to Whisk. This highlights ARTv2's
10 potential to automatically detect whiskers which have low spatial resolution. Whisk also had a high
11 false positive rate, with scratches on the arena floor and parts of the animal's fur being detected as
12 whiskers. These false positives may occur because Whisk was designed for use on head restrained
13 rodents with only a single row of whiskers on either side (Clack et al., 2012).

14
15 The ARTv2 whisker detector is comparable to BWTT for tracking whiskers in freely moving animals
16 with intact whiskers. It is also fully-automated, whereas BWTT is only semi-automated and required
17 manual intervention for the settings. Although ARTv2 performed as well as BWTT on the Z2 dataset
18 (Table 2), it detected a significantly higher amount of *TP* whiskers on the Z1 dataset. It should also be
19 noted that all the settings in ARTv2 are dynamically computed for each individual frame. BWTT
20 manual settings can have a major impact on whisker detection rates (Figure 8). These settings are
21 then applied across an entire video, meaning if the rodent were to travel from an area of high
22 brightness into an area of low brightness, which is common, the program may begin to fail to detect
23 whiskers. ARTv2 would continue to operate at the same detection rate regardless of brightness
24 variation. We used only one image per video for validation, which mean BWTT was manually set up
25 exactly for that frame, and all other frames are likely to degrade from there.

26 *Foot detection*

27 As well as a fully automated whisker detection, we also present a foot tracking algorithm that is able
28 to correctly label, and detect feet from monochrome footage which is collected to detect whiskers
29 of small rodents (Grant et al., 2018a). The foot detector in ARTv2 was not validated against any
30 other software, due to either the software not being open source (Herold et al., 2016), dependent
31 on two views ((Kloefkorn et al., 2017) or being unable to track feet within the monochrome video
32 (Mendes et al., 2015). However, against manual annotation of still images, it was possible to obtain
33 an *IoU* score of 0.502. It is also possible from the outputs generated from this tracker, to calculate
34 stride length, swing speed, swing time, stance time, for each foot, and even the possibility to present
35 pixel intensity maps for a visual representation on how much pressure the animal is applying to the
36 ground.

37 The mean *IoU* score obtained by ARTv2 foot detector highlights the potential benefits of using ARTv2
38 to automatically annotate and record gait information for videos. It also has the benefit of reducing
39 the time needed to annotate a full video manually with software such as Supervisely (Supervise.ly,
40 2019) or MWA (Hewitt et al., 2016). The *IoU* score for the foot detector is relatively low, which could
41 be due to a number of reasons. This includes the ground truth bounding boxes lying outside the area
42 of the body, and the number of parameters used to fine-tune the foot tracking affecting the *IoU*
43 score. Finally, *IoU* treats errors the same in small bounding boxes and large bounding boxes. A small
44 error in a large predicted or ground truth bounding box is generally benign but a small error in a
45 small predicted or ground truth bounding box has a much greater effect on the *IoU* score. This could

1 also explain why the *IoU* values for mouse were much lower for the rat data. However, the
2 difference in *IoU* between rat and mouse could also be due to the settings creating artefacts, or
3 erroneously eroding features needed to identify feet.

4 *Locowhisk System outputs*

5 The mean statistics of the outputs from ARTv2, are consistent with data previously recorded for rat
6 and mice. The mean whisker frequency for rats (11.04 ± 5.08 Hz) and mice (19.49 ± 8.02 Hz) are
7 similar to what was recorded in Mitchinson et al. (2011) (8.55 ± 0.62 Hz and 11.35 ± 0.95 Hz,
8 respectively) and Grant et al. (2018a) (8.8 ± 0.76 Hz and 16.08 ± 7.05 Hz, respectively). The
9 protraction speed recorded in ARTv2 for both species (1.434 ± 0.51 deg/ms and 1.535 ± 0.79
10 deg/ms) is very similar to values recorded in Grant et al. (2018a) (1.34 ± 0.1 and 1.69 ± 0.31 ,
11 respectively). However the retraction speeds of rats and mice (1.274 ± 0.51 deg/ms, 1.535 ± 0.79
12 deg/ms respectively) are higher than those recorded in Grant et al. (2018a) (0.15 ± 0.05 deg/ms,
13 0.43 ± 0.23 deg/ms, respectively). The whisker amplitude for rats and mice ($24.2 \pm 9.30^\circ$, 17.36 ± 4.47
14 $^\circ$ respectively) is much smaller than values in Grant et al. (2018a), yet is similar to the model
15 calculated amplitude ($29.19 \pm 7.14^\circ$, $16.21 \pm 6.49^\circ$, respectively) in Mitchinson et al. (2011). The
16 mean whisker angles recorded in ARTv2 were very similar in both species. However, Mitchinson et
17 al. (2011) and Grant et al. (2018a), found that the mouse whisker angle (or offset) is often lower in
18 rats. Differences in whisker measurements, could be due to individual differences in both whisker
19 movements or locomotion, as whisker movements and positioning is associated with locomotion
20 speed (Arkley et al. 2014).

21 Results from the ARTv2 foot detector are also similar to data from the literature. The recorded
22 mean stride distance for rats and mice for fore (101.5 ± 42.0 mm, 56.95 ± 10.3 mm) and hind (48.52
23 ± 0.0 mm, 51.42 ± 13.93 mm) feet respectively in ARTv2, are very similar to fore feet data from
24 Santos et al. (1995) of 113 mm for rats and mice of 66-70 mm (Amende et al., 2005; Virmouni et al.,
25 2014). The animals in this study were filmed in a free and open environment, rather than a treadmill
26 or trackway; therefore, there is probably some differences in gait, especially in the timing. Indeed,
27 rats in this study have slightly longer stance (fore: 302.0 ± 89.75 ms, hind: 365.4 ± 248.7 ms) and
28 swing times (385.2 ± 130.8 ms) for their forefeet, compared to data from Santos et al. (1995)
29 (stance: 200ms, swing:130 ms) and Herold et al. (2016). The mouse stance times (fore: 131.7 ± 34.38
30 ms, hind: 171.3 ± 72.28 ms) are similar to those recorded in Mendes et al., (2015). Although the
31 swing phase of the mice feet in this study are slightly longer (fore: 498.3 ± 374.0 ms, hind: $216.3 \pm$
32 40.42 ms) than those recorded in Mendes et al., (2015). This could be due to a number of factors,
33 such as the animals exploring and interacting with elements within the LocoWhisk arena, such as
34 objects and walls. Measurements of gait recorded in the literature are usually conducted either on a
35 treadmill, trackway or in tunnel. These approaches do not necessarily represent coordinated
36 movements and locomotion seen in freely moving and exploring rodents (Herbin et al., 2007; Batka
37 et al., 2014; Guillot et al., 2008). Therefore, the LocoWhisk arena and software (ARTv2) might
38 encourage more natural locomotion behaviours and gaits than some other experimental set-ups.

39 The whisker and foot tracking algorithms incorporated into ARTv2, have been designed to be
40 automated and reduce manual intervention while maintaining accuracy levels similar to that of
41 other methods, particularly on datasets with low spatial resolution. ARTv2, has been designed to be
42 usable by researchers who have little to no programming expertise, and is freely available as an
43 executable file with a Graphical User Interface (GUI) at: <https://github.com/AIEMMU/ARTv2>. The
44 source code is also available for researchers to reproduce the results in this paper, explore the code
45 base and expand upon our current work (from: <https://github.com/AIEMMU/ARTv2>).

1 *Conclusion*

2

3 We demonstrate within this paper that the LocoWhisk arena and ARTv2 are able to detect feet and
4 whiskers accurately. The LocoWhisk system and ARTv2 represent the first step in developing a
5 robust, fully-automated whisker and foot detector for detecting whiskers and feet in freely moving
6 rodents in a range of experimental conditions, including open-field and during object exploration.
7 The whisker detection algorithm has been developed as an alternative to existing whisker detectors.
8 It has been designed to reduce as much manual intervention as possible, while maintaining accuracy
9 levels similar to that of other methods. This was achieved by dynamically calculating each required
10 setting per frame, and can thus be used on datasets consisting of various brightness and contrast
11 changes. The foot tracking algorithm has been developed with a similar ethos to reduce user
12 interaction, and to be usable on other datasets of varying brightness. Both achieve robust and
13 accurate detection compared to manual tracking. Future software development may include
14 incorporating machine learning algorithms, or integrating behavioural tracking with
15 electrophysiology or electromyography measurements. This would enable musculoskeletal or neural
16 measurements to be collected alongside behavioural assessments.

17

18 The LocoWhisk arena can robustly measure rodent whisker movements and gait. It can be applied to
19 rodent models to help us to better understand how disease progression can affect motor control,
20 which may lead to the development of new rodent models and the design of new treatments.

21

22 **Acknowledgements**

23 We would like to thank Antonello Mallamachi and Marco Stebel for providing access to the opossum
24 colony at the University of Trieste animal facility, and to Hazel Ryan and Vicki Breakell for their
25 continued support and access to animals at the Wildwood Trust. We are grateful to Tony Prescott,
26 Ben Mitchinson and Kendra Arkley at the University of Sheffield for their support producing the pilot
27 set-up, which first combined whisker filming with a pedobarograph.

28 **References**

29 Ahissar, E. and Knutsen, P. M. (2008) 'Object localization with whiskers.' *Biological cybernetics*, 98(6)
30 pp. 449-458.

31

32 Arkley, K., Grant, R. A., Mitchinson, B. and Prescott, T. J. (2014) 'Strategy change in vibrissal active
33 sensing during rat locomotion.' *Current Biology*, 24(13) pp. 1507-1512.

34

35 Bale, M. R., Campagner, D., Erskine, A. and Petersen, R. S. (2015) 'Microsecond-scale timing precision
36 in rodent trigeminal primary afferents.' *Journal of Neuroscience*, 35(15) pp. 5935-5940.

37

38 Bradski, G. and Kaehler, A. (2008) *Learning OpenCV: Computer vision with the OpenCV library*. "
39 O'Reilly Media, Inc."

40

41 Clack, N. G., O'Connor, D. H., Huber, D., Petreanu, L., Hires, A., Peron, S., Svoboda, K. and Myers, E.
42 W. (2012) 'Automated tracking of whiskers in videos of head fixed rodents.' *PLoS computational*
43 *biology*, 8(7) p. e1002591.

44

45 Corr, S., McCorquodale, C. and Gentle, M. (1998) 'Gait analysis of poultry.' *Research in veterinary*
46 *science*, 65(3) pp. 233-238.

1
2 Dauchy, R. T., Wren, M. A., Dauchy, E. M., Hoffman, A. E., Hanifin, J. P., Warfield, B., Jablonski, M. R.,
3 Brainard, G. C., Hill, S. M. and Mao, L. (2015) 'The influence of red light exposure at night on
4 circadian metabolism and physiology in Sprague–Dawley rats.' *Journal of the American Association*
5 *for Laboratory Animal Science*, 54(1) pp. 40-50.

6
7 Devernay, F. (1995) *A non-maxima suppression method for edge detection with sub-pixel accuracy.*
8 INRIA.

9
10 Garland, H., Wood, N. I., Skillings, E. A., Detloff, P. J., Morton, A. J. and Grant, R. A. (2018)
11 'Characterisation of progressive motor deficits in whisker movements in R6/2, Q175 and Hdh knock-
12 in mouse models of Huntington's disease.' *Journal of neuroscience methods*, 300 pp. 103-111.

13
14 Gonzalez, R. C. and Woods, R. E. (2002) 'Thresholding.' *Digital Image Processing*, pp. 595-611.

15
16 Grant, R. A., Mitchinson, B. and Prescott, T. J. (2012) 'The development of whisker control in rats in
17 relation to locomotion.' *Developmental psychobiology*, 54(2) pp. 151-168.

18
19 Grant, R. A., Breakell, V. and Prescott, T. J. (2018a) 'Whisker touch sensing guides locomotion in
20 small, quadrupedal mammals.' *Proceedings of the Royal Society B: Biological Sciences*, 285(1880) p.
21 20180592.

22
23 Grant, R. A., Mitchinson, B., Fox, C. W. and Prescott, T. J. (2009) 'Active touch sensing in the rat:
24 anticipatory and regulatory control of whisker movements during surface exploration.' *Journal of*
25 *neurophysiology*, 101(2) pp. 862-874.

26
27 Grant, R. A., Haidarliu, S., Kennerley, N. J. and Prescott, T. J. (2013) 'The evolution of active vibrissal
28 sensing in mammals: evidence from vibrissal musculature and function in the marsupial opossum
29 *Monodelphis domestica*.' *Journal of Experimental Biology*, 216(18) pp. 3483-3494.

30
31 Grant, R. A., Wong, A. A., Fertan, E. and Brown, R. E. (2018b) 'Whisker exploration behaviours in the
32 5xFAD mouse are affected by sex and retinal degeneration.' *Genes, Brain and Behavior*, p. e12532.

33
34 Grant, R. A., Sharp, P. S., Kennerley, A. J., Berwick, J., Grierson, A., Ramesh, T. and Prescott, T. J.
35 (2014) 'Abnormalities in whisking behaviour are associated with lesions in brain stem nuclei in a
36 mouse model of amyotrophic lateral sclerosis.' *Behavioural brain research*, 259 pp. 274-283.

37
38 Grant, R. A., Cielen, N., Maes, K., Heulens, N., Galli, G. L., Janssens, W., Gayan-Ramirez, G. and
39 Degens, H. (2016) 'The effects of smoking on whisker movements: A quantitative measure of
40 exploratory behaviour in rodents.' *Behavioural processes*, 128 pp. 17-23.

41
42 He, K., Gkioxari, G., Dollár, P. and Girshick, R. (2017) *Mask r-cnn*.

43

1 Herold, S., Kumar, P., Jung, K., Graf, I., Menkhoff, H., Schulz, X., Bähr, M. and Hein, K. (2016) 'CatWalk
2 gait analysis in a rat model of multiple sclerosis.' *BMC neuroscience*, 17(1) p. 78.

3

4 Hewitt, B., Yap, M. H. and Grant, R. A. (2016) 'Manual whisker annotator (mwa): A modular open-
5 source tool.' *Journal of Open Research Software*, 4(1)

6

7 Hewitt, B. M., Yap, M. H., Hodson-Tole, E. F., Kennerley, A. J., Sharp, P. S. and Grant, R. A. (2018) 'A
8 novel automated rodent tracker (ART), demonstrated in a mouse model of amyotrophic lateral
9 sclerosis.' *Journal of neuroscience methods*, 300 pp. 147-156.

10

11 Kloefkorn, H. E., Pettengill, T. R., Turner, S. M., Streeter, K. A., Gonzalez-Rothi, E. J., Fuller, D. D. and
12 Allen, K. D. (2017) 'Automated Gait Analysis Through Hues and Areas (AGATHA): a method to
13 characterize the spatiotemporal pattern of rat gait.' *Annals of biomedical engineering*, 45(3) pp. 711-
14 725.

15

16 Knutsen, P. M., Derdikman, D. and Ahissar, E. (2005) 'Tracking whisker and head movements in
17 unrestrained behaving rodents.' *Journal of neurophysiology*, 93(4) pp. 2294-2301.

18

19 Lin, T.-Y., Goyal, P., Girshick, R., He, K. and Dollár, P. (2017) *Focal loss for dense object detection*.

20

21 Mendes, C. S., Bartos, I., Márka, Z., Akay, T., Márka, S. and Mann, R. S. (2015) 'Quantification of gait
22 parameters in freely walking rodents.' *BMC biology*, 13(1) p. 50.

23

24 Mitchinson, B., Grant, R. A., Arkley, K., Rankov, V., Perkon, I. and Prescott, T. J. (2011) 'Active vibrissal
25 sensing in rodents and marsupials.' *Philosophical Transactions of the Royal Society B: Biological
26 Sciences*, 366(1581) pp. 3037-3048.

27

28 O'Connor, D. H., Clack, N. G., Huber, D., Komiyama, T., Myers, E. W. and Svoboda, K. (2010) 'Vibrissa-
29 based object localization in head-fixed mice.' *Journal of Neuroscience*, 30(5) pp. 1947-1967.

30

31 Pammer, L., O'Connor, D. H., Hires, S. A., Clack, N. G., Huber, D., Myers, E. W. and Svoboda, K. (2013)
32 'The mechanical variables underlying object localization along the axis of the whisker.' *Journal of
33 Neuroscience*, 33(16) pp. 6726-6741.

34

35 Peirson, S. N., Brown, L. A., Potheary, C. A., Benson, L. A. and Fisk, A. S. (2018) 'Light and the
36 laboratory mouse.' *Journal of neuroscience methods*, 300 pp. 26-36.

37

38 Perkon, I., Košir, A., Itskov, P. M., Tasič, J. and Diamond, M. E. (2011) 'Unsupervised quantification of
39 whisking and head movement in freely moving rodents.' *Journal of Neurophysiology*, 105(4) pp.
40 1950-1962.

41

42 Real, R. and Vargas, J. M. (1996) 'The probabilistic basis of Jaccard's index of similarity.' *Systematic
43 biology*, 45(3) pp. 380-385.

44

1 Redmon, J., Divvala, S., Girshick, R. and Farhadi, A. (2016) *You only look once: Unified, real-time*
2 *object detection*.

3

4 Rosenfeld, A. (1976) *Digital picture processing*. Academic press.

5

6 Sofroniew, N. J., Cohen, J. D., Lee, A. K. and Svoboda, K. (2014) 'Natural whisker-guided behavior by
7 head-fixed mice in tactile virtual reality.' *Journal of Neuroscience*, 34(29) pp. 9537-9550.

8

9 Supervise.ly. (2019) *The leading platform for entire computer vision lifecycle: Iterate from image*
10 *annotation to accurate neural networks 10x faster*. [Online] [Accessed on 01/02/2019]

11

12 Technology, N. I. (2012) *CatWalk XT Version 10.0. Reference Manual*. Noldus Information
13 Technology b.v. , Wageningen, The Netherlands.

14

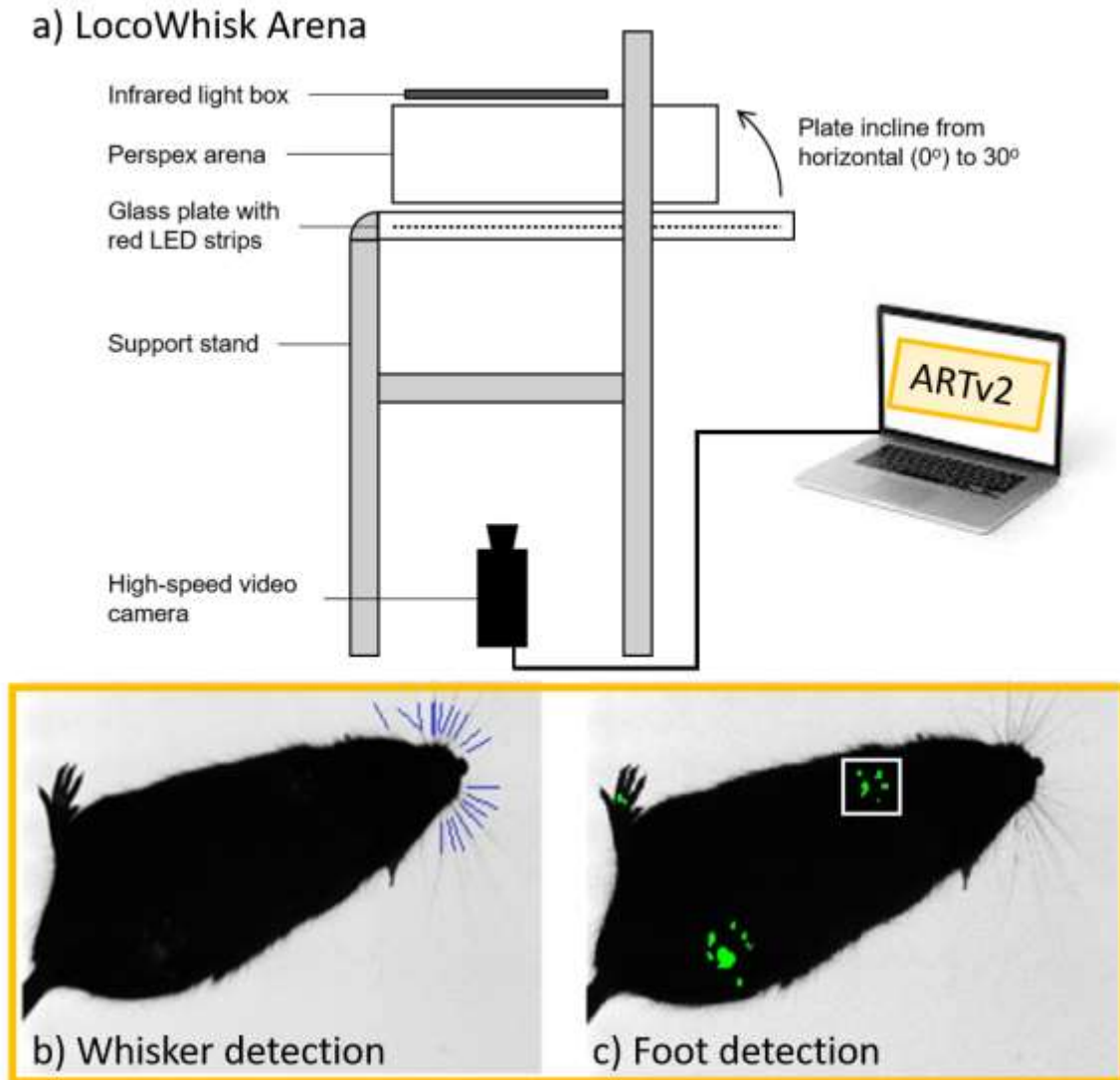
15 Voigts, J., Sakmann, B. and Celikel, T. (2008) 'Unsupervised whisker tracking in unrestrained behaving
16 animals.' *Journal of neurophysiology*, 100(1) pp. 504-515.

17

18

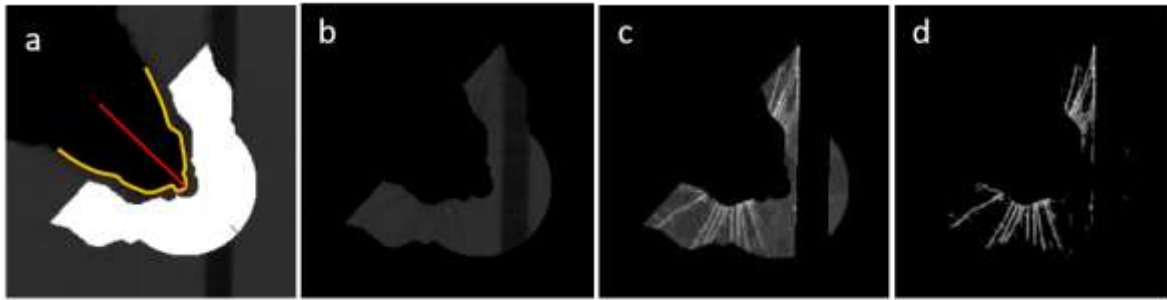
19

1 FIGURE CAPTIONS



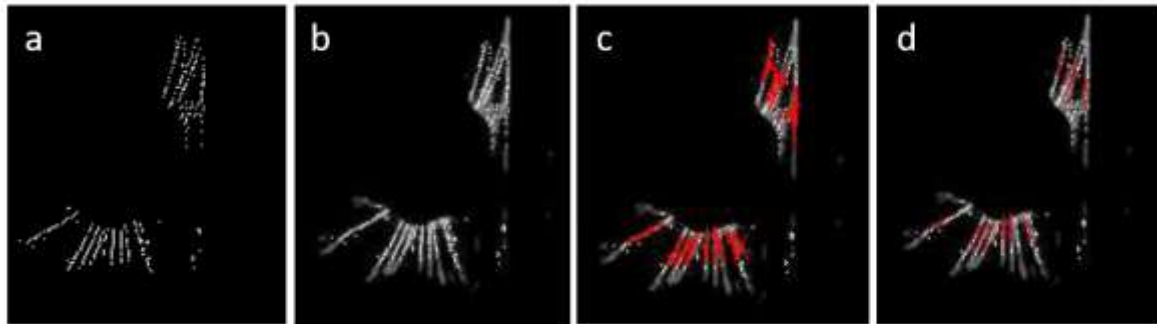
2
3
4
5
6
7
8

Fig. 1: The LocoWhisk Arena and ARTv2 software. (a) schematic of arena; (b) Inset: Example high-speed video footage, showing overlaid whisker detection; and (c) foot detection.



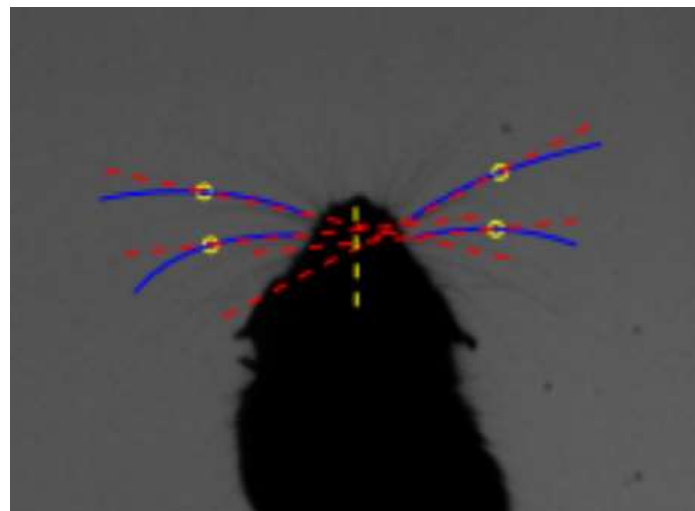
1
2
3
4
5

Fig. 2: Illustration of the ROI image enhancement stages. a) The computed ROI mask; b) ROI extraction; c) Linear Normalisation; and d) Threshold to zero.



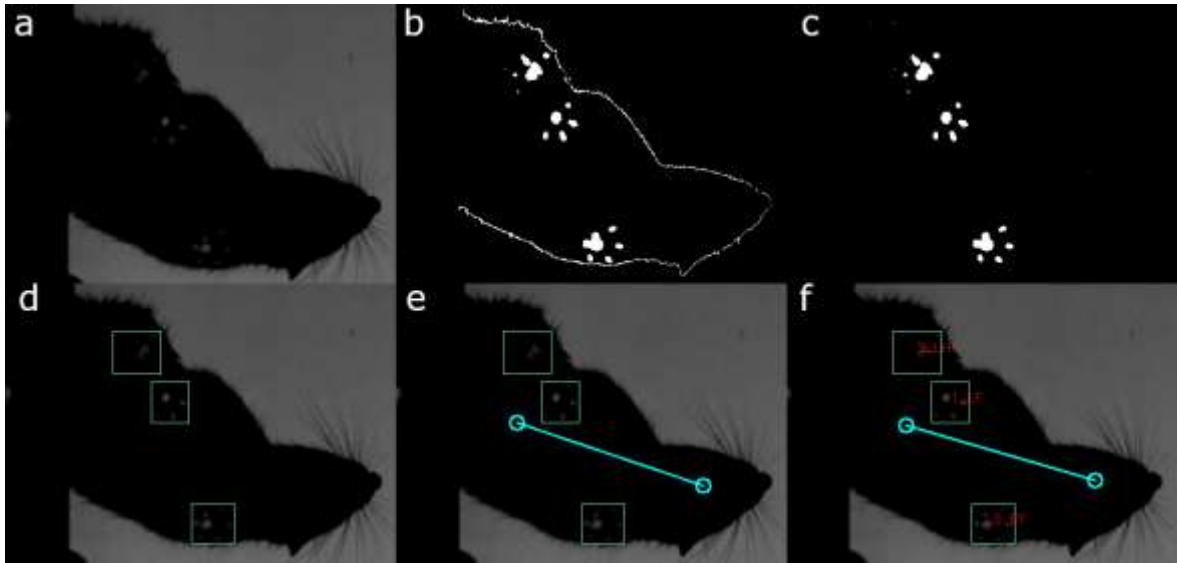
6
7
8
9
10

Fig. 3: An overview of the whiskers localisation and detection. a) Probable whisker locations; b) Probably whisker locations added to the ROI image; c) All potential whisker lines; and d) The detected whiskers.



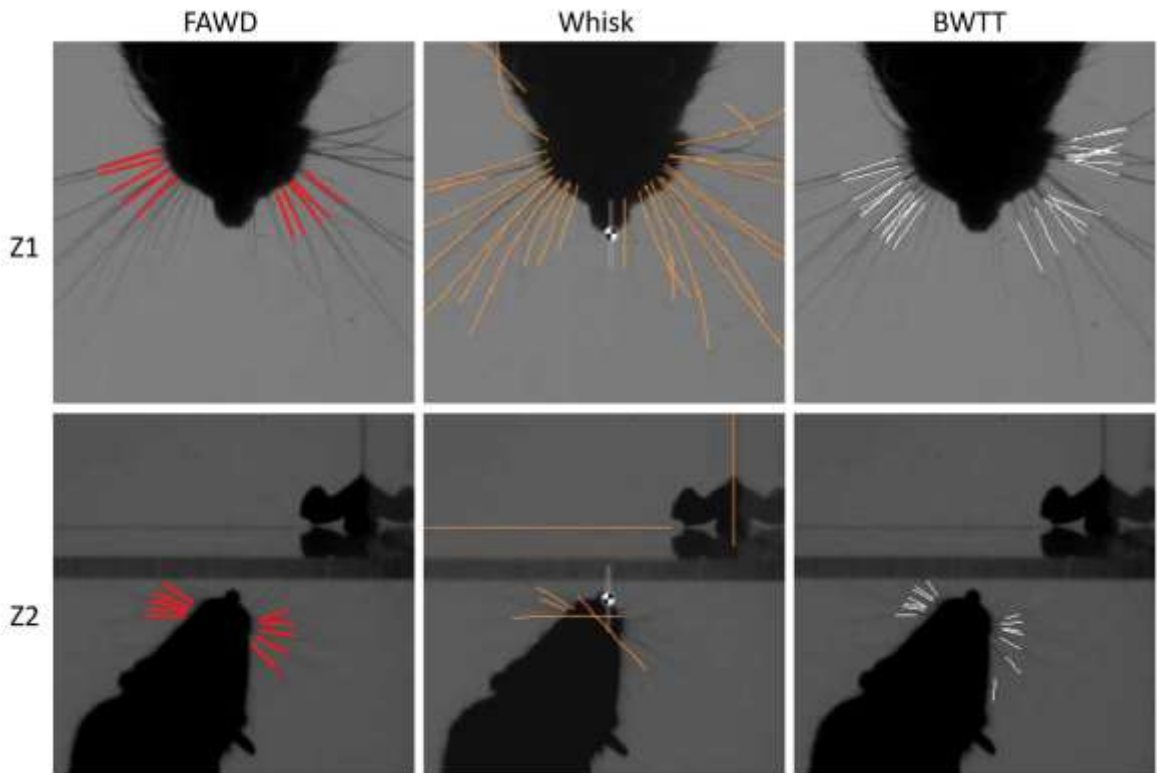
11
12
13
14

Fig. 4: Whisker angular positions. The whisker angle is calculated by taking the tangent from the midline of the rodent's head to a point on a given whisker shaft.



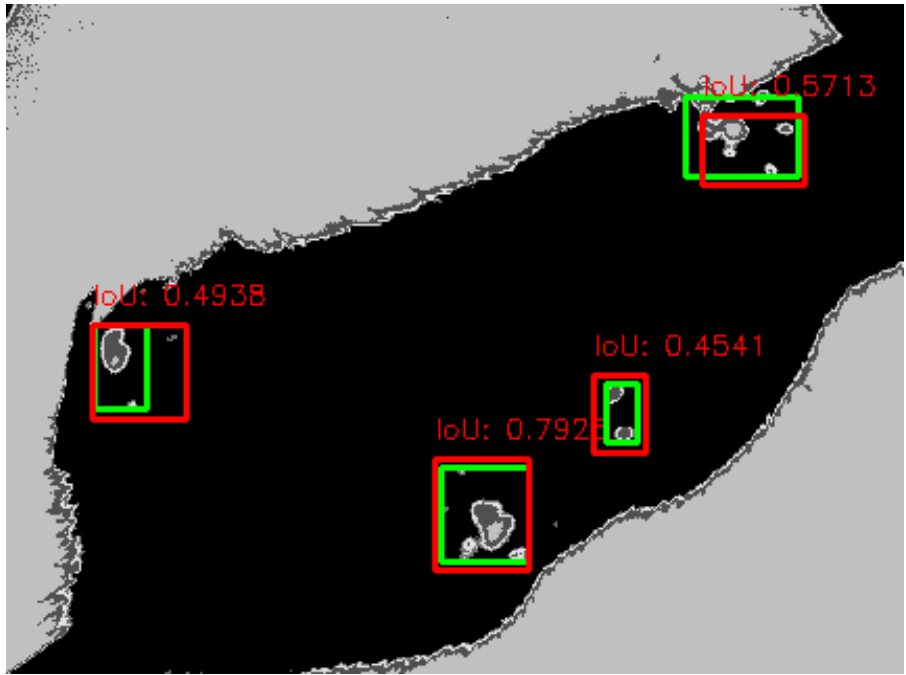
1
2
3
4
5
6
7

Fig. 5: Visual illustration of the proposed foot detection algorithm. a) Input frame from a video; b) Mask created by segmenting the body from the image and converting to the log colour space; c) Eroded mask; d) Foot bounding boxes; e) Bounding boxes and the line splitting the rodent; f) Correctly labelled feet.



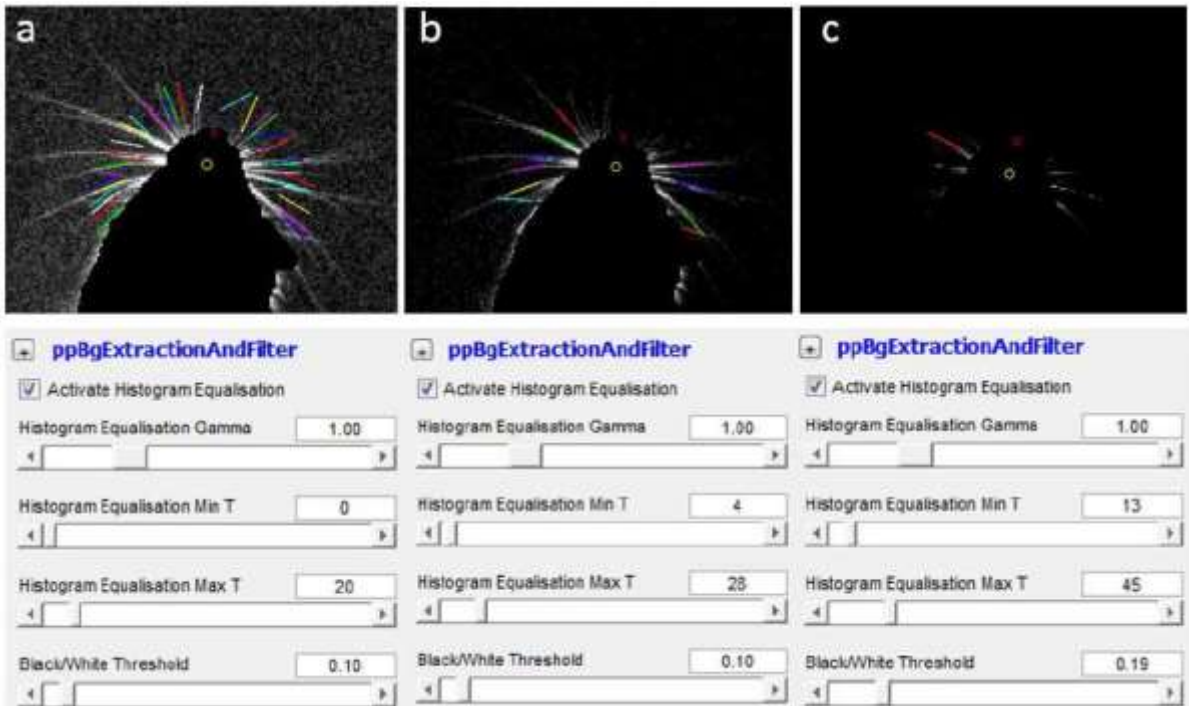
8
9
10
11

Fig. 6: Comparison of different whisker detectors on two different Zoom levels. The first column is Artv2, the 2nd is Whisk and the 3rd is BWTT. The first row (a) is a higher-resolution dataset; the Bottom: b) is a lower resolution dataset.



1
2
3
4

Fig. 7: An example of image, with the predicted *IoU* score for each foot print. Green boxes are ground truth annotations and red boxes are predicted boxes.



5
6
7

Fig. 8: Variation in detection rates for different settings in BWT